V International Conference on Computational Methods for Coupled Problems in Science and Engineering
COUPLED PROBLEMS 2013
S. Idelsohn, M. Papadrakakis and B. Schrefler (Eds)

COUPLED THERMOELASTIC SIMULATION OF NANOVOID CAVITATION BY DISLOCATION EMISSION AT FINITE TEMPERATURE

M. PONGA[†], M. ORTIZ[‡] AND M.P. ARIZA[*]

[*]Escuela Técnica Superior de Ingeniería, Universidad de Sevilla
Camino de los descubrimientos, s.n. 41092-Sevilla, Spain
E-mail: mpariza@us.es, http://personal.us.es/mpariza/

[†] Mechanical and Civil Engineering, California Institute of Technology,
1200 E. California Blvd. Pasadena, 91125 CA, USA.
E-mail: mponga@caltech.edu

[‡] Graduate Aeronautical Laboratories, California Institute of Technology,
1200 E. California Blvd. Pasadena, 91125 CA, USA.
E-mail: ortiz@aero.caltech.edu

Key words: Multiscale modeling, Crystal plasticity, Thermomechanical coupling, Nanovoids, Dislocations

Abstract. In this work we study the early onset of void growth by dislocation emission at finite temperature in single crystal of copper under uniaxial loading conditions using the HotQC method. The results provide a detailed characterization of the cavitation mechanism, including the geometry of the emitted dislocations, the dislocation reaction paths and attendant macroscopic quantities of interest such as the cavitation pressure. In addition, this work shows that as prismatic dislocation loops grow and move away from the void, the material surrounded by these loops is pushed away from the void surface, giving rise to a flux of material together with a heat flux through the crystal.

1 INTRODUCTION

Crystal defects play a critical role in determining macroscopic properties of solids, even when they are presented in small concentrations [1, 2]. Defects such as vacancies and nanovoids, modify the perfection of the crystal lattice and produce changes in different scales of length and time. The void nucleation mechanism is usually followed by plastic cavitation when the void attains the critical size for dislocation emission. Furthermore, the dissipation of this plastic work generates thermal fields around the nanovoid that fosters localization of deformation and mass transport by self-diffusion through dislocation cores

[3]. This coupling between mass transport and heat flux occurs on multiple time and length scales. As a result, the study of this type of problems must reproduce the coupled nature of the thermoelastic response of the material as well as their mustiscale nature.

One multiscale approach which enables us to simulate thermomechanical coupled problems such as void cavitation and crack tip opening, among others, is the Quasicontinuum method (QC). This method was proposed fifteen years ago [4] as a multiscale modeling approach for the solution of mechanical problems where atomistic resolution is required in a localized subset of the domain under analysis. Initially, the QC was applied to the solution of mechanical problems in solids with defects at $0K$. More recently, the method has been extended to encompass non-equilibrium coupled thermomechanical problems [5, 3], enabling the full analysis of continuum/atomistic domains at finite temperature and away from equilibrium. This extension is called HotQC method and has been applied to different plasticity problems such as nanoindentation [5] and nanovoid growth under triaxial load [3]. The development of the HotQC method for non-homogeneous temperature distributions relies on three main considerations. Firstly, the instantaneous vibrations of the atoms are eliminated through the use of the Jayne's principle of maximum entropy [6], by performing phase averages and formulating a mean field free energy in terms of the macroscopic atomic variables, i. e., position, temperature and frequency. Secondly, a variational thermoelastic formulation proposed by Yang *et al.* [7] is required in order to describe equilibrium and non-equilibrium processes. Third, a coarse-graining model of the material allows bridging the continuum and atomistic scales. The method starts with a small and complete atomistic system around a core defect. One of the main advantages of the HotQC methodology, is that we can simulate systems in different thermodynamic states, varying from isothermal to adiabatic states. In this work, we study the evolution of void growth in copper single crystals at finite temperature under uniaxial load using the HotQC method.

2 SIMULATION DETAILS

The simulations performed in this work were carried out using the following set up. The representative volume Ω_{RV} is a cubic box of dimensions $(72a_0)^3$ of Cu simulated using the EAM-type potential proposed by Mishin *et al.* [8]. Since the publication of our preliminary results [9, 10] where we used a different EAM potential, we have observed that the results present a high dependency on the interatomic potential used to perform the simulation. Even though this discussion is beyond the scope of this paper, we would like to mention that it is mostly due to the stacking fault energies predicted by each interatomic potential. In the center of the volume a full atomistic zone, which is a cube of dimensions $(14a_0)^3$, is defined. A spherical void of $12a_0$ diameter is modeled in the center of Ω_{RV}, by removing atoms from the initial atomistic zone. Away from the full representative zone we apply systematically coarsening of the sample Ω_{RV} using a set of representative atoms or nodes. Therefore, a Finite Element (FE) mesh is constructed using a Delaunay triangulation over the nodes. Previously to loading process the sample

is allowed to relaxed at an initial temperature $T_0 = 300K$, this is performed by the minimization of the mean field free energy with respect to nodal positions and frequencies. For the thermal expansion, the Boundary Conditions (BC) applied to the sample consist on fixing the normal displacement of the atoms in planes $x = 0$, $y = 0$ and $z = 0$. This BC ensures isothermal expansion of the crystal without distortion.

After the thermal expansion, the computational cell is deformed applying a homogeneous deformation gradient to simulate a uniaxial load in [001] direction, where the deformation increment is set as 0.1%. Hence, we impose dilatational displacements on the external boundaries, i. e., at $z = \pm 36a_0$ and find the equilibrium positions of the remaining ones by minimizing the mean field free energy. In every deformation step, an equilibrium configuration is found using a nonlinear conjugate gradient [11], or alternatively dynamic relaxation method is used [12, 13, 14] when the computational minimization process during a certain loading step becomes very slow. In addition, the temperature is allowed to change between steps of deformation and its equilibrium value for each atom is reached by using a nonlinear conjugate gradient algorithm. Finally, in order to capture all the emitted dislocations surrounding the void, we implement a routine that automatically remeshes the sample using the second invariant of the deviatoric part of the Lagrangian strain tensor as adaptivity indicator. In this work, we focus on the detailed analysis of dislocations patterns emitted from the void surface at high strain rate load, $\dot{\epsilon} = 10^{10}s^{-1}$, typical of molecular dynamics calculations, and the evolution of the atomic temperature during the process.

3 RESULTS

In a previous publication [3], we have estimated the range of strain rates for which microinertia is expected to play a significant role during void growth. Our findings were consistent with foregoing continuum analysis and suggested that inertia is negligible for small enough voids. Based on this, we restrict attention for the present to quasistatic HotQC calculations.

Figure 1 shows the evolution of the virial stress *vs* strain, as well as the void fraction (V_{void}/V_{sample}) for an initial temperature of $300K$ and strain rate $\dot{\epsilon} = 10^{10}s^{-1}$. We distinguish four main stages in the virial stress evolution: i) an initial elastic regimen up to the cavitation of the void at $\epsilon = 6.5\%$, characterized by the elastic expansion of the void without the emission of dislocations, ii) a second and third plastic stages where dislocations are emitted from the void surface and which extend up to $\epsilon = 9.0\%$ and $\epsilon = 13.0\%$, respectively, and finally, iii) a fourth stage characterized by loss of stiffness up to ductile failure of the crystal. The deformation mechanisms which dominates the void growth under uniaxial load are revealed in details in the following section.

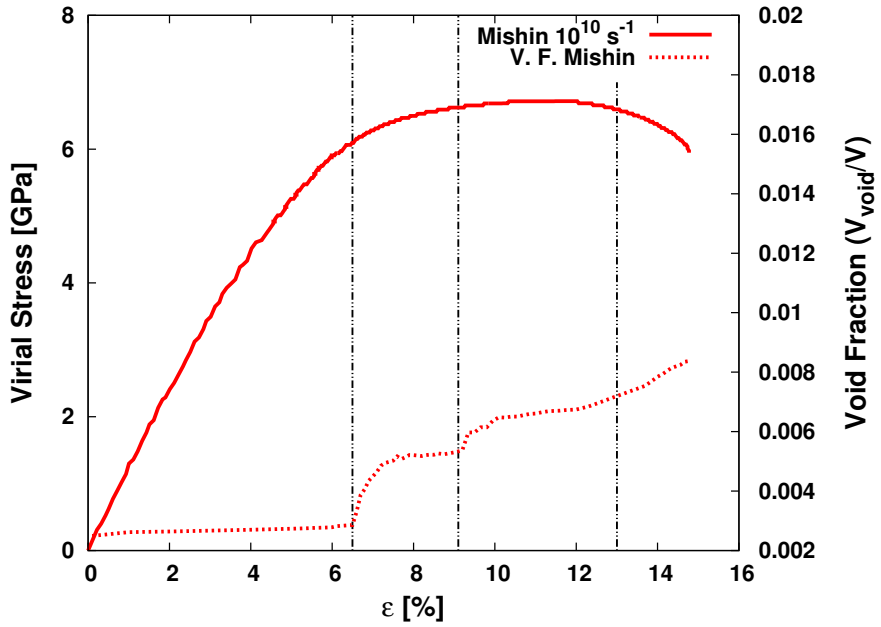

Figure 1: Virial stress *vs* strain and void fraction for single crystal copper predicted by HotQC using Mishin potential for a simulation sample of size $72a_0^3$ and void of radius 2.2 nm.

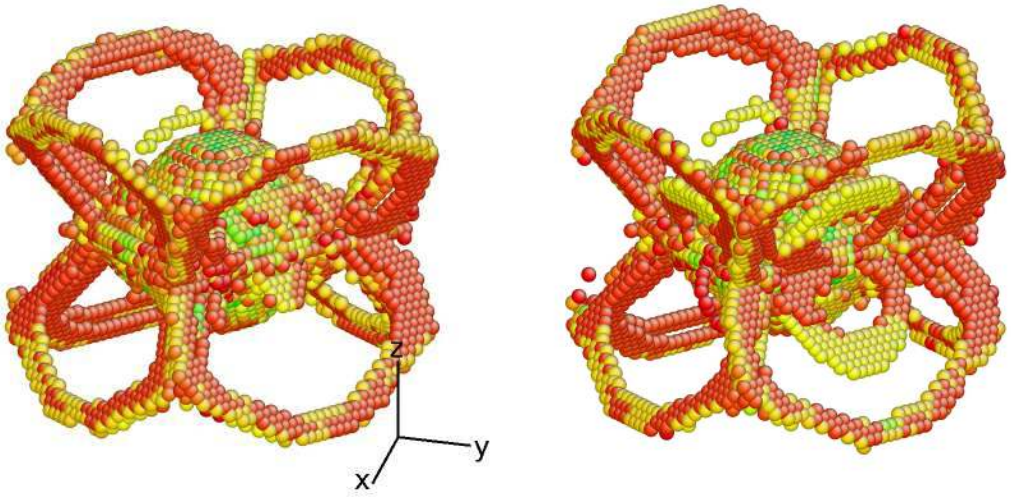

(a) Shockley partial dislocations at $\epsilon = 6.8\%$. (b) Trailing edge dislocations at $\epsilon = 7.0\%$.

Figure 2: Dislocations emission from the void surface for uniaxial loading case. (a) Shockley partial dislocations with Burgers vector $1/6\langle 211\rangle$ emitted from the void at $\epsilon = 6.8\%$. (b) Trailing dislocations of the first ones are emitted at $\epsilon = 7.0\%$.

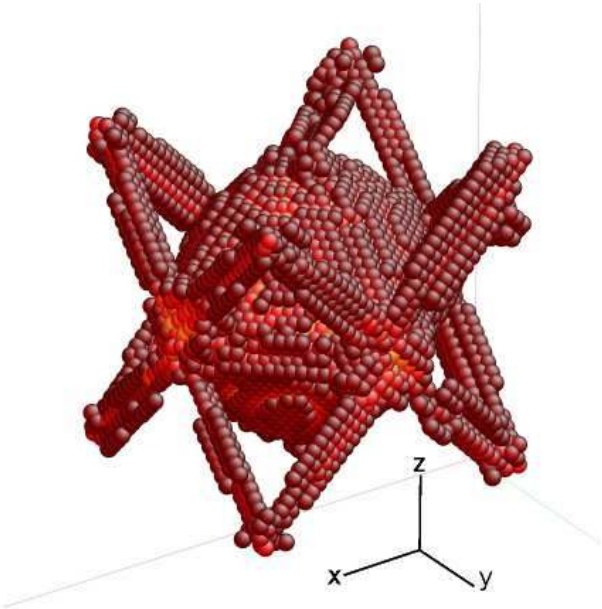

Figure 3: Lomer-Cottrell dislocations emitted from the void surface at $\epsilon = 8.5\%$. ($T_0 = 300K$ and $\dot{\epsilon} = 10^{10}s^{-1}$).

Dislocations Emission

The virial stress *vs* strain curve (Figure 1) presents a linear behaviour up to $\epsilon = 6.5\%$. Throughout this first stage, the void is mostly deformed along the loading direction and no significant transversal deformation is observed. However, as the strain attains the value of 6.6%, the critical stress for cavitation is reached, and therefore, we start observing dislocation emission from the equator of the void ($z = 0$). This first set of eight stacking fault dislocations grow on planes $\{111\}$ with Burgers vector $1/6\langle 211\rangle$. In this sense, due to its shorter Burgers vector, Shockley partial dislocations are energetically more favourable than other type of dislocations [15, 16]. The Burgers vectors of the leading Shockley partial dislocations emitted are

Table 1: Leading dislocations emitted from void surface

z positive axis		z negative axis	
$Z1:$	$1/6[\overline{1}\overline{1}2]$	$Z5:$	$1/6[\overline{1}\overline{1}2]$
$Z2:$	$1/6[\overline{1}\overline{1}2]$	$Z6:$	$1/6[\overline{1}\overline{1}2]$
$Z3:$	$1/6[\overline{1}\overline{1}2]$	$Z7:$	$1/6[\overline{1}\overline{1}2]$
$Z4:$	$1/6[\overline{1}\overline{1}2]$	$Z8:$	$1/6[\overline{1}\overline{1}2]$

Figure 2a shows the set of leading dislocations emitted at $\epsilon = 6.8\%$. As the energy of the Shockley partial dislocations is lower than any other type of dislocation, the stacking fault plane expands outward easily. In addition, during this plastic growth regime, a second set of Shockley partial dislocations is emitted from the void surface, which are the trailing edge dislocation of the first set, as we can see in Figure 2b. However, the shear stress in the crystal decreases proportionally to $1/r^2$ from the void surface [17] and consequently the driving force needed to move the set of stacking fault planes also decreases. Hence, these stacking fault planes decelerate giving rise to different dislocation structures. Therefore, additional shear loops with $1/6\langle 211\rangle$ Burgers vector are emitted from the void along the perpendicular direction to the loading direction. These shear loops join at the intersection of planes $x = \pm z$ with $x_0 = \pm R_0$ and $y = \pm z$ with $y_0 = \pm R_0$ to form a Lomer-Cottrell dislocation at $\epsilon = 8.5\%$. Figure 3 shows the atoms comprising the void surface together with the Lomer-Cottrell dislocations that remain attached to its surface. For instance, dislocation reactions on the $x = R_0$ plane might be summarized as

$$\begin{aligned} X1: &\quad 1/6[1\bar{2}\bar{1}] + 1/6[12\bar{1}] \rightarrow 1/3[10\bar{1}] \\ X2: &\quad 1/6[121] + 1/6[1\bar{2}1] \rightarrow 1/3[101] \\ X3: &\quad 1/6[12\bar{1}] + 1/6[1\bar{2}\bar{1}] \rightarrow 1/3[10\bar{1}] \\ X4: &\quad 1/6[121] + 1/6[1\bar{2}1] \rightarrow 1/3[101] \end{aligned} \tag{1}$$

The Lomer-Cottrell dislocations form a rhombus shape and constitute the starting point for the emission of four Prismatic Dislocation Loops (PDL) along directions $\langle 110\rangle$. The mechanism underlying the emission of the PDLs along the $\langle 110\rangle$ directions is as follows: first, two shear loops are emitted form the void surface on two different planes, such as $(\bar{1}11)$ and $(1\bar{1}1)$. Following these two shear loops, another two are also emitted on the same planes to form the rhomboidal shape which characterizes the PDLs (see Figure4b). The complete reactions for the shear loops into prismatic ones are

$$\begin{aligned} &1/6[\bar{2}11] + 1/6[\bar{2}1\bar{1}] + 1/6[\bar{1}21] + 1/6[\bar{1}2\bar{1}] \rightarrow [\bar{1}10] \\ &1/6[\bar{2}\bar{1}1] + 1/6[\bar{2}11] + 1/6[\bar{1}2\bar{1}] + 1/6[\bar{1}21] \rightarrow [\bar{1}\bar{1}0] \\ &1/6[1\bar{2}1] + 1/6[1\bar{2}\bar{1}] + 1/6[2\bar{1}1] + 1/6[2\bar{1}\bar{1}] \rightarrow [1\bar{1}0] \\ &1/6[211] + 1/6[12\bar{1}] + 1/6[21\bar{1}] + 1/6[121] \rightarrow [110] \end{aligned} \tag{2}$$

Figure 4 shows the complete sequence of dislocation patterns, including the emission of stacking faults and PDLs at different values of deformation. Finally, when the strain reaches $\epsilon = 13\%$, the crystal gradually loss stiffness ending with the ductile failure at about $\epsilon = 15\%$.

(a) Dislocations at $\epsilon = 8.0\%$.

(b) Dislocations at $\epsilon = 9.0\%$.

(c) Dislocations at $\epsilon = 10.0\%$.

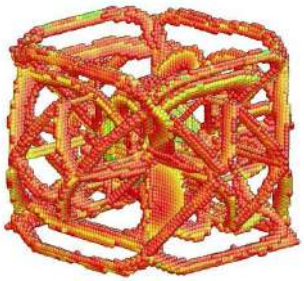

(d) Dislocations at $\epsilon = 11.0\%$.

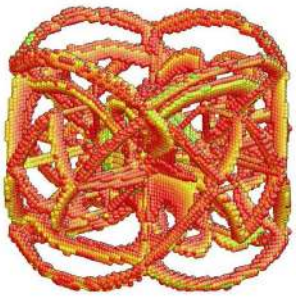

(e) Dislocations at $\epsilon = 12.0\%$.

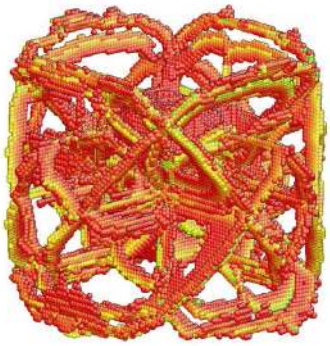

(f) Dislocations at $\epsilon = 13.0\%$.

Figure 4: Dislocations emission from the void surface as the deformation increases. The snapshots are taken for 8.0% to 13.0% at steps of 1.0% of deformation. The load is applied in the vertical direction. All figures have the same scale. ($T_0 = 300K$ and $\dot{\epsilon} = 10^{10}s^{-1}$).

Temperature Evolution

Figure 5a shows the time evolution of the temperature at three different points within the crystal: one point on the surface of the void, a second point near to the void and a third point far from the void. Before attaining the critical strain for dislocation emission $\epsilon = 6.5\%$, the crystal cools down due to the thermoelastic effect as expected for large strain rates. This variation in the temperature is clearly linear in consequence with the linear deformation of the crystal. However, when the deformation within the sample reaches the critical value for dislocations emission, the temperature in the vicinity of the void surface increases. The highest temperature is reached at the void surface and the increase is about $20K$. Figure 5b shows the temperature field of plane $z = 0$ for a deformation of $\epsilon = 7.0\%$. We clearly observe that the temperature field after dislocations emission is inhomogeneous and varies notably near to the void surface. Figure 5b also shows other important behaviour in the evolution of the atomic temperatures, showing how the atomic temperature increases when one PDL is passing through the atom labelled as "Near to the void" (located around $5\sigma_0$ from void surface in [110] direction). The increment of the atomic temperature due to dislocations emission indicates that as the PDLs move away the material surrounded by the dislocation loops is pushed away from the void surface, giving rise to a flux of material together with a heat flux through the crystal. Finally, when deformation reaches about 12.0% the temperature homogenizes within the crystal and continues cooling down up to the end of the simulation.

Void Growth

Figure 6a shows the initial configuration of the void at $T_0 = 300K$. At this point, the void is a discrete sphere of radius $r_0 = 6.0a_0$. When the sample is deformed the void starts growing elastically in the loading direction up to the first yield point at $\epsilon = 6.5\%$ and no transversal growth is observed, as we can see in Figure 6b. After this point, the critical strain for dislocations emission is reached and dislocations arise from the void surface. A detailed description of the evolution of the void growth as a function of the applied strain helps us to understand the mechanism of deformation underlying this loading condition. In fact, Figure 6c shows that the void grows in the direction perpendicular to the applied load in order to relax the internal energy of the crystal which causes the emission of dislocations. This mechanism has been predicted before based on continuum theory of spherical void growth and is known as *prolate-to-oblate* transition (see [18] and references therein). Finally, as deformation increases, the atoms comprising the surface of the void change their position and the void adopts an octahedral shape (see Figure 6f). This effect has also been observed in MD simulations performed by [19] where they attribute the octahedral shape to several factor such as: the low surface energy of the {111} surfaces common in fcc metals, the high anisotropy of the copper elastic constants and the {111} dislocation glide systems.

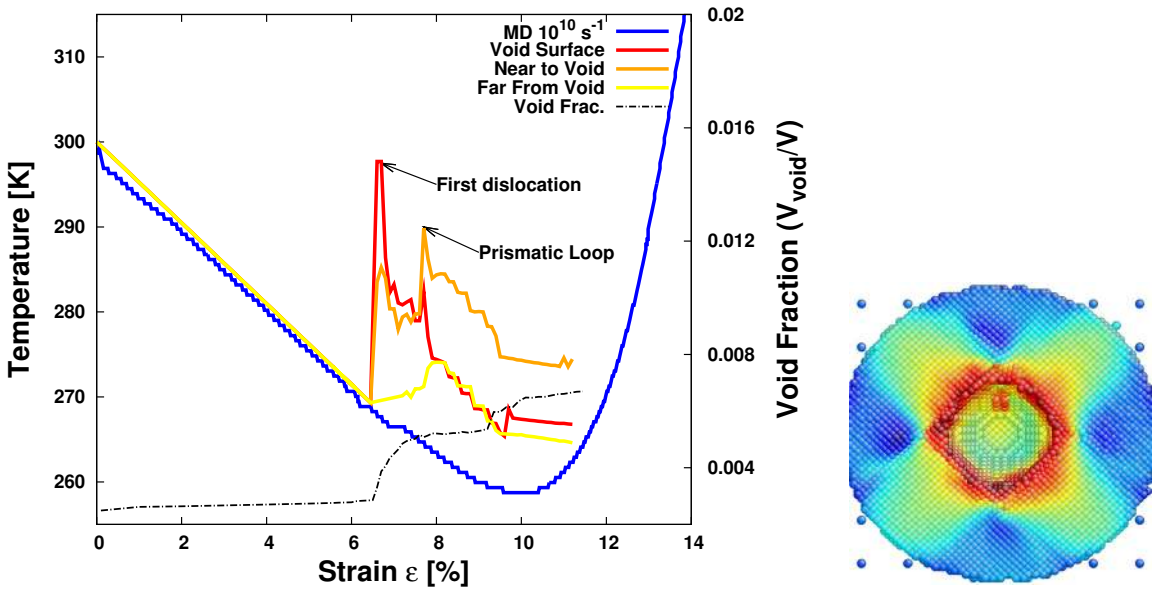

(a) Temperature evolution with ϵ.

(b) Temperature field along $z = 0$.

Figure 5: (a) Temperature evolution at different position within the crystal: void surface, near to the void surface and far from the void surface. Void fraction is also plotted. (b) Temperature field for $\epsilon = 7.0\%$ along the plane $z = 0$. Results obtained for $T_0 = 300K$ and $\dot{\epsilon} = 10^{10} s^{-1}$.

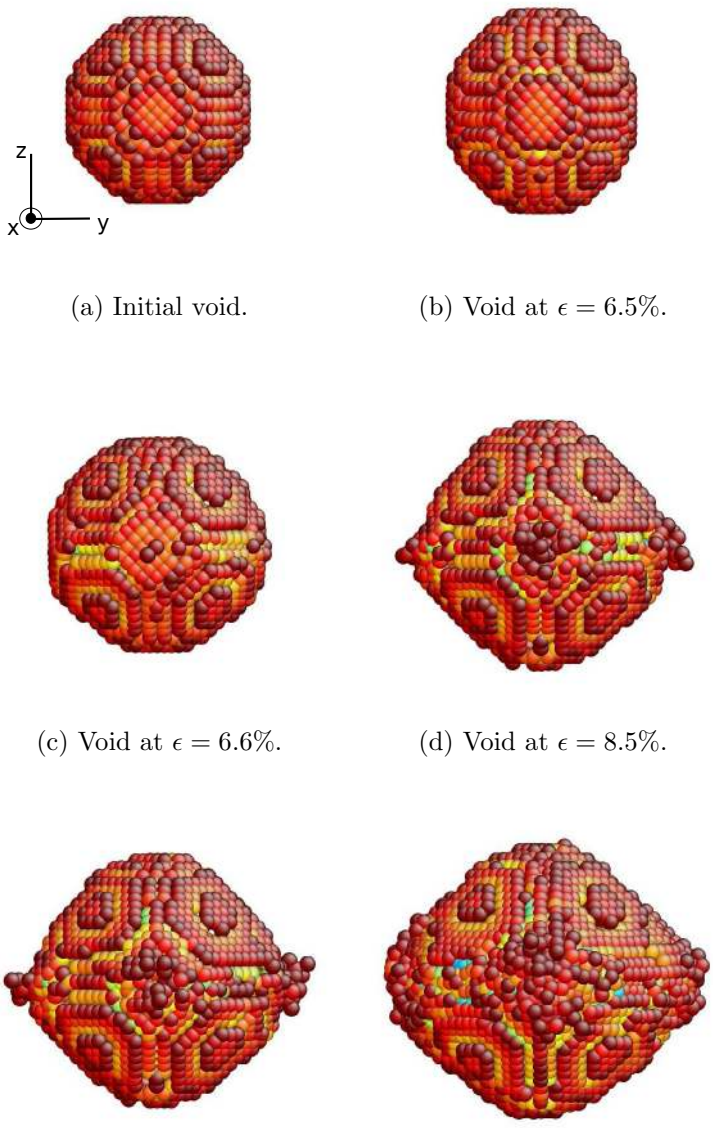

(a) Initial void.

(b) Void at $\epsilon = 6.5\%$.

(c) Void at $\epsilon = 6.6\%$.

(d) Void at $\epsilon = 8.5\%$.

(e) Void at $\epsilon = 10.0\%$.

(f) Void at $\epsilon = 12.0\%$.

Figure 6: Void growth under uniaxial loading conditions. ($T_0 = 300K$ and $\dot{\epsilon} = 10^{10}s^{-1}$). All figures have the same scale.

4 CONCLUSIONS

We have applied the HotQC method [5] to the study of quasistatic void growth in copper single crystals at finite temperature under uniaxial expansion using the EAM-type potential proposed by Mishin *et al.* [8]. We find that, upon the attainment of a critical or cavitation strain of the order of $\epsilon = 6.5\%$, dislocations are abruptly and profusely emitted from the void surface and the rate of growth of the void increases rapidly in directions perpendicular to the loading direction. The simulation carried out in this work shows the emission of four PDLs in $\langle 110 \rangle$ directions. This effect is called *prolate to ablate* and has also been observed in MD simulations [19] as well as for void growth using continuum mechanics [18]. Regarding the temperature field within the sample, prior to cavitation, the crystal cools down due to the thermoelastic effect. By contrast, dislocations emission after cavitation causes a rapid local heating in the vicinity of the void, which in turn sets up a temperature gradient and results in the conduction of heat away from the void. This result indicates that the problem of void growth at finite temperature need to be performed using a coupled computational tool, such as HotQC method, which allows us the study of both thermodynamic and plastic evolution of the crystal.

5 Acknowledgements

We gratefully acknowledge the support of the Ministerio de Ciencia e Innovación of Spain (DPI2009-14305-C02-01) and the support of the Consejería de Innovación of Junta de Andalucía (P09-TEP-4493). Support for this study was also provided by the Department of Energy National Nuclear Security Administration under Award Number DE-FC52-08NA28613 through Caltech's ASC/PSAAP Center for the Predictive Modeling and Simulation ofHigh Energy Density Dynamic Response of Materials.

REFERENCES

[1] R. Martin, *Electronic Structure: Basic theory and practical methods*. Cambridge University Press, 2004.

[2] M. Finnis, *Interatomic Forces in Condensed Matter*. Oxford Series on Materials Modelling 1, Oxford University Press, 2003.

[3] M. P. Ariza, I. Romero, M. Ponga, and M. Ortiz, "Hotqc simulation of nanovoid growth under tension in copper," *International Journal of Fracture*, vol. 174, pp. 75–85, 2012.

[4] E. B. Tadmor, M. Ortiz, and R. Phillips, "Quasicontinuum analysis of defects in solids," *Philosophical Magazine*, vol. 73, pp. 1529–1563, 1996.

[5] Y. Kulkarni, J. Knap, and M. Ortiz, "A variational approach to coarse graining of equilibrium and non-equilibrium atomistic description at finite temperature," *Journal of the Mechanics and Physics of Solids*, vol. 56, pp. 1417–1449, 2008.

[6] E. Jaynes, "Information theory and statistical mechanics," *Physical Review*, vol. 106, pp. 620–630, 1957.

[7] Q. Yang, L. Stainier, and M. Ortiz, "A variational formulation of the coupled thermo-mechanical boundary-value problem for general dissipative solids," *Journal of the Mechanics and Physics of Solids*, vol. 54, pp. 401–424, 2006.

[8] Y. Mishin, M. Mehl, D. Papaconstantopoulos, A. Voter, and J. Kress, "Structural stability and lattice defects in copper: Ab initio, tight-binding, and embedded-atom calculations," *Physical Review B*, vol. 63, no. 22, 2001.

[9] M. P. Ariza, M. Ponga, I. Romero, and M. Ortiz, "Finite-temperature nanovoid deformation in copper under tension," in *Computational Plasticity XI: Fundamentals and Applications* (Onate, E and Owen, DRJ and Peric, D and Suarez, B, ed.), pp. 1517–1526, 2011.

[10] M. Ponga, I. Romero, M. Ortiz, and M. P. Ariza, "Finite temperature nanovoids evolution in fcc metals using quasicontinuum method," *Key Engineering Materials*, vol. 488-489, pp. 387–390, 2012.

[11] W. T. Vetterling, W. H. Press, B. P. Flannery, and S. A. Teukolsky, *Numerical Recipes Example Book C++*. Cambridge University Press, 2002.

[12] D. R. Oakley and N. F. Knight, "Adaptive dynamic relaxation algorithm for non-linear hyperelastic structures part i. formulation," *Computer Methods in Applied Mechanics and Engineering*, vol. 126, no. 1-2, pp. 67 – 89, 1995.

[13] D. R. Oakley, N. F. Knight, and D. D. Warner, "Adaptive dynamic relaxation algorithm for non-linear hyperelastic structures part iii. parallel implementation," *Computer Methods in Applied Mechanics and Engineering*, vol. 126, no. 1-2, pp. 111 – 129, 1995.

[14] P. Underwood, *Computational methods for transient analysis, Belytschko, T. and Hughes, T.J.R.* Computational methods in mechanics, North-Holland, 1983.

[15] J. P. Hirth and J. Lothe, *Theory of Dislocations, 2nd New edition of Revised edition.* Krieger Publishing Company, 1991.

[16] D. Hull and D. J. Bacon, *Introduction to dislocations.* Butterworth-Heinemann, 2001.

[17] J. Marian, J. Knap, and M. Ortiz, "Nanovoid cavitation by dislocation emission in aluminum," *Physical Review Letters*, vol. 93, no. 16, 2004.

[18] P. Ponte Castañeda and M. Zaidman, "Constitutive models for porous materials with evolving microstructures.," *Journal of the Mechanics and Physics of Solids*, vol. 42, pp. 1459–1497, 1994.

[19] E. Seppälä, J. Belak, and R. Rudd, "Effect of stress triaxiality on void growth in dynamic fracture of metals: A molecular dynamics study," *Physical Review B*, vol. 69, no. 13, p. 134101, 2004.